Title

Gene therapy into photoreceptors and Müller glial cells restores retinal structure and function in CRB1 retinitis pigmentosa mouse models.

Journal

Human molecular genetics, 24(11)

ISSN

0964-6906

Authors

Pellissier, Lucie P
Quinn, Peter M
Alves, C Henrique
et al.

Publication Date

2015-06-01

DOI

10.1093/hmg/ddv062

Peer reviewed

OXFORD

Human Molecular Genetics, 2015, Vol. 24, No. 11 3104–3118

doi: 10.1093/hmg/ddv062
Advance Access Publication Date: 20 February 2015
Original Article

ORIGINAL ARTICLE

Gene therapy into photoreceptors and Müller glial cells restores retinal structure and function in *CRB1* retinitis pigmentosa mouse models

Lucie P. Pellissier[1], Peter M. Quinn[1], C. Henrique Alves[1], Rogier M. Vos[1], Jan Klooster[2], John G. Flannery[4], J. Alexander Heimel[3] and Jan Wijnholds[1,5,*]

[1]Department of Neuromedical Genetics, [2]Department of Retinal Signal Processing and [3]Department of Cortical Structure & Function, Netherlands Institute for Neuroscience, an Institute of the Royal Netherlands Academy of Arts and Sciences, 1105 BA Amsterdam, The Netherlands, [4]Department of Molecular and Cellular Biology, The Helen Wills Neuroscience Institute, University of California, Berkeley, CA, USA and [5]Department of Ophthalmology, Leiden University Medical Center, 2300 RC Leiden, The Netherlands

*To whom correspondence should be addressed at: Department of Neuromedical Genetics, Netherlands Institute for Neuroscience, 1105 BA Amsterdam, The Netherlands. Tel: +31 205664597; Fax: +31 205666121; Email: j.wijnholds@nin.knaw.nl

Abstract

Mutations in the *Crumbs-homologue-1* (*CRB1*) gene lead to severe recessive inherited retinal dystrophies. Gene transfer therapy is the most promising cure for retinal dystrophies and has primarily been applied for recessive null conditions via a viral gene expression vector transferring a cDNA encoding an enzyme or channel protein, and targeting expression to one cell type. Therapy for the human CRB1 disease will be more complex, as CRB1 is a structural and signaling transmembrane protein present in three cell classes: Müller glia, cone and rod photoreceptors. In this study, we applied *CRB1* and *CRB2* gene therapy vectors in *Crb1*-retinitis pigmentosa mouse models at mid-stage disease. We tested if CRB expression restricted to Müller glial cells or photoreceptors or co-expression in both is required to recover retinal function. We show that targeting both Müller glial cells and photoreceptors with *CRB2* ameliorated retinal function and structure in *Crb1* mouse models. Surprisingly, targeting a single cell type or all cell types with *CRB1* reduced retinal function. We show here the first pre-clinical studies for *CRB1*-related eye disorders using CRB2 vectors and initial elucidation of the cellular mechanisms underlying CRB1 function.

Introduction

Mutations in the *Crumbs-homologue-1* (*CRB1*) gene cause severe autosomal recessive retinal dystrophies, chronic and disabling vision disorders, and are the genetic cause of the visual defect in approximately 80 000 patients worldwide (1). CRB1-related retinal dystrophies range from the congenital blindness Leber congenital amaurosis (LCA8) to early onset and heterogeneous retinitis pigmentosa (RP) and display features common to many forms of RP as well as some unique clinical features such as pigmented paravenous chorioretinal atrophy, macular atrophy alone, retinal degeneration associated with Coats disease, para-arteriolar preservation of the retinal pigment epithelium or nanophthalmia (1,2). To date, over 150 mutations have been identified in the entire exome and all protein domains of CRB1, there is no clear correlation between the type or location of these mutations and the clinical presentation (3).

In mammals, the complex and large *CRB1* gene belongs to a family of three genes, *CRB1*, *CRB2* and *CRB3*. CRB1 and CRB2 proteins have a large extracellular domain composed of epidermal growth factor and laminin-globular domains, a single transmembrane domain, and a short intracellular domain with FERM and PDZ binding domains, which interact with members of the CRB

Received: December 9, 2014. **Revised and Accepted:** February 13, 2015

complex (1). CRB2 is highly similar to CRB1 but shorter than CRB1, whereas CRB3 lacks the extracellular domain and has two alternative splicing variants (CRB3A and CRB3B). CRB proteins localize to the subapical region, above the adherens junctions between photoreceptor–photoreceptor and between photoreceptor–Müller glial cells. In human retinas, CRB1 at the subapical region is expressed above the adherens junctions in Müller glial cells and cone and rod photoreceptors, while CRB2 is localized at the subapical region only in Müller glial cells (4).

In mice, the protein expression pattern is reversed, as Crb1 is expressed only in Müller glial cells and Crb2 in both photoreceptors and Müller glial cells (5). Knockout *Crb1*$^{-/-}$, knockin *Crb1*$^{C249W/-}$ and naturally occurring *Crb1*$^{rd8/rd8}$ mice show mild retinal disorganization limited to one quadrant of the inferior retina (6–9). *Crb2* conditional knockout (cKO) in retinas results in severe, progressive degeneration throughout the retina due to essential functions of Crb2 in photoreceptors (10–12). *Crb1Crb2*$^{F/+}$ cKO retinas display severe, rapid degeneration in the entire inferior retina with impaired retinal function and are together with *Crb2* cKO good mouse models of *CRB1*-RP (4). *Crb1*$^{+/-}$*Crb2* and *Crb1Crb2* cKO retinas showed increased number of proliferative cells, severe lamination defects with ectopic localization of retinal cells and rapidly lose retinal electrical responses and are good mouse models of *CRB1*-LCA (13). *Crb1*, *Crb2* and *Crb1Crb2* cKO mouse models show phenotypes ranging from mild RP to severe LCA. Crb2 is a modifying factor of *Crb1*-retinal dystrophies in mice (4). Crb1 and Crb2 proteins have been shown to have similar functions in adult mice and are involved in the lamination of the retina and the maintenance of the adherens junctions between photoreceptors and Müller glial cells (1,4,6,10,13). These proteins also serve to restrain the number of progenitor cells and control Notch and Hippo signaling pathways (10,13).

Over the last six years, clinical trials of adeno-associated virus (AAV) gene replacement therapies for *RPE65 (LCA2)*, *CHM*-REP1, *MERTK* and *VEGFR1/FLT-1* genes have shown the greatest promise to prevent human retinopathies, LCA, choroideremia, RP and exudative age-related macular degeneration respectively (14–20).

Most of these studies involved gene transfer to a single cell type (in most cases, retinal pigment epithelium) and transgenes with short (under 4 kb) coding sequences encoding enzymes, channels or secreted factors. Developing an AAV-mediated gene therapy for *CRB1*-related retinal diseases is more challenging due to (a) the large *CRB1* cDNA (4.2 kb) which approaches the AAV packaging limit, (b) a disorder affecting three different cell types, rods, cones and Müller glial cells and (c) the complex functions of CRBs, as structural and signaling transmembrane proteins (1). It has been suggested that it might be difficult to package *CRB1* cDNA in AAV vectors due to the size of the cDNA (21). Recently, we showed that the use of short promoters and polyadenylation sequence allow efficient packaging of human *CRB1* cDNA in AAV vectors at high titer and to efficient CRB1 expression *in vivo* (22). In this study, we used successfully another approach to bypass the AAV size limitation, choosing the human *CRB2* cDNA, which is highly similar in homology and function but smaller than *CRB1*. We showed that recombinant human CRB2 protein located correctly in the mouse retina at the subapical region. Then, we performed rescue experiments with *CRB1* and *CRB2* vectors in already severely disorganized retina of *Crb1Crb2*$^{F/+}$ cKO and *Crb2* cKO animals, our two *CRB1*-RP mouse models and tested the hypothesis if targeting of only Müller glial cells or photoreceptors or both are necessary to ameliorate retinal function. We found that only *CRB2* targeted in both Müller glial cells and photoreceptors prevented further loss of retinal function in our two mouse models. Surprisingly, *CRB1* had adverse effects on retinal activity in retinas lacking endogenous Crb1, whereas overexpression of CRB1 or CRB2 in retinas expressing endogenous mouse Crb1 and Crb2 did not lead to loss of retinal activity or structure. In this study, we showed the first report of amelioration of retinal function and structure in *CRB1*-RP mice.

Results

Efficient expression of CRB2 proteins upon AAV gene transfer

Previously, we showed by inclusion of short promoters (350 bp maximum) and a small synthetic poly-adenylation sequence in combination with the full-length human *CRB1* cDNA (4.2 kb) that the size limitation of AAV vectors can be accommodated, resulting in efficient packaging and high titer vectors (22). Following subretinal injection, CRB1 protein was expressed at the subapical region in *Crb1*$^{-/-}$ retinas (22). The other alternative to bypass the AAV size limitation is the use of the most similar but shorter Crumbs family member, human *CRB2* (3.85 kb; Supplementary Material, Fig. S1A). CRB2 proteins are expressed at the subapical region in WT retinas but are not found in *Crb2* cKO retinas (Fig. 1A and B). In contrast to *CRB1*, we found that human CRB2 expressed efficiently *in vitro* in ARPE-19 cell lines (Supplementary Material, Fig. S1B). We previously proved that subretinal applied AAV9 targets Müller glial and photoreceptor cells (and retinal pigment epithelium; 22). Using subretinal injection of AAV9-CMV-*CRB2*, CRB2 protein was mainly found at the subapical region of Müller glial cells and photoreceptors, and at the apical membrane of retinal pigment epithelium (white arrowheads, Fig. 1C). Following subretinal injection of AAV9-hGRK1-*CRB2*, which directs expression exclusively to rods and cones, CRB2 protein was located at the subapical region (white arrowhead), primarily at the tip of the inner segments and minimally in their somata (Fig. 1D). We previously showed that the AAV-ShH10Y targets mainly Müller glial cells but not photoreceptors via the intravitreal route (22). Intravitreal injection of ShH10Y-CMV-*CRB2*, resulted in CRB2 protein expression only at the subapical region (white arrowhead) of Müller glial cells (Fig. 1E).

In summary, by careful selection of AAV serotype, promoter choice and surgical route of administration, human CRB2 proteins can be efficiently expressed at the subapical region of *Crb2* cKO retinas *in vivo*.

Targeting human *CRB2* in both Müller glial cells and photoreceptors ameliorated retinal function and structure in CRB1-RP mouse models

We showed previously and in this study that cellular targets for *CRB1*-related gene therapy are both Müller glial cells and rod and cone photoreceptors (4). Here, we tested if targeting of human *CRB1* or *CRB2* in only Müller glial cells, photoreceptors or both would suffice to rescue retinal degeneration in mid-stage *CRB1*-RP mouse models. To address this question, we developed tools to target specifically Müller glial cells (intravitreal injection of ShH10Y capsid vectors with CMV or minCMV promoters), cone and rod photoreceptors (subretinal injection of vectors with GRK1 promoter) and both Müller glial cells and photoreceptors (subretinal injection of AAV9 capsid vectors with CMV or minCMV promoters) (22).

Crb2 cKO and *Crb1Crb2*$^{F/+}$ cKO, two *CRB1*-RP mouse models, showed impairment of retinal function and structure postnataly from 1 and 3 months onwards, respectively (4,10). Here, we tested the potential rescue activity of AAV vectors expressing *CRB2* in the two mouse models at mid-stage of the disease and performed

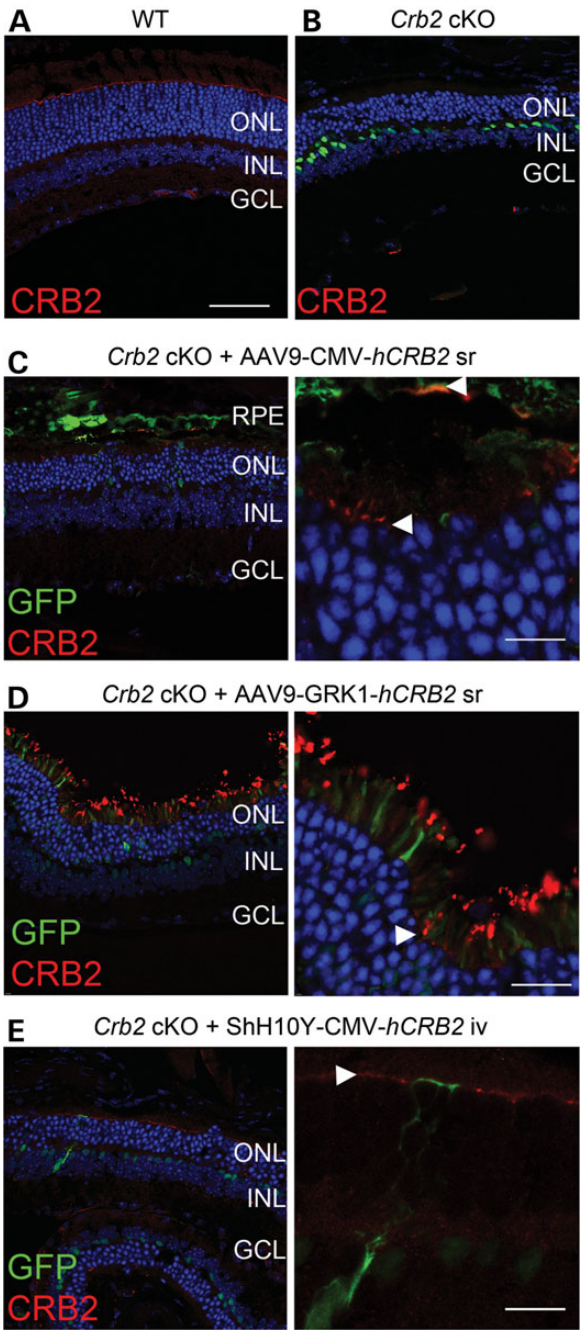

Figure 1. Efficient expression of human CRB2 after AAV-*CRB2* injection in *Crb2* cKO retinas. Mouse CRB2 expressed at the subapical region in WT retinas (**A**) and did not express in *Crb2* cKO retinas (**B**). After three weeks post-injection in *Crb2* cKO retinas of 2.10^{10} genome copies of either subretinally AAV2/9-CMV-*CRB2* (targeting photoreceptors, Müller glial cells and RPE; **C**) and AAV2/9-hGRK1-*hCRB2* (targeting exclusively photoreceptors; **D**) or intravitreally AAV2/ShH10Y-CMV-*CRB2* (targeting Müller glial cells; **E**) in addition to 10^9 genome copies of the respective GFP virus, CRB2 protein was detected at the subapical region for the three vectors (white arrowheads) and in the apical membrane of RPE cells only with the CMV promoter subretinally (white arrowheads in C). Surprisingly, when targeting only photoreceptors (D), human CRB2 expression was mainly found at the tip of the inner segment of photoreceptors whereas targeting photoreceptors and Müller glial cells (C), CRB2 expressed mainly at the subapical region. *Crb2* cKO retinas displayed Cre-GFP positive bipolar cells due to the Chx10 promoter. GCL, ganglion cell layer; INL, inner nuclear layer; iv, intravitreal; ONL, outer nuclear layer; RPE, retinal pigment epithelium; sr, subretinal. $n = 2$–4/viral vector. (C–E) Right panels, zoom-in of left panels. Scale bar: 50 µm (A left, B right, C left, D left, E left), 10 µm (C right, D right, E right).

AAV injections at post-natal day (P) 14. Retinal function was performed by ERG equipment that measured a maximum b-wave amplitude of about 250 µV in wild type and control $Crb2^{F/F}$. Improvement of retinal function in all *CRB2*-injected *Crb2* cKO eyes (subretinal 2.10^{10} viral particles AAV9-CMV-*CRB2*; Fig. 2A and B) was observed as an increased amplitude a-wave, indicative of photoreceptor function (*CRB2* 30 ± 7 µV versus *GFP* 10 ± 3 µV) and increased b-wave amplitudes which corresponds to ON bipolar cell function (*CRB2* 84 ± 11 µV versus *GFP* 43 ± 10 µV). Similarly, maximal amplitudes for the scotopic a-wave (*CRB2* 52 ± 6 µV versus *GFP* 34 ± 8 µV), scotopic b-wave (*CRB2* 158 ± 13 µV versus *GFP* 107 ± 33 µV) and photopic b-wave (*CRB2* 36 ± 4 µV versus *GFP* 14 ± 8 µV, $P = 0.045$) were all higher in *CRB2*-treated $Crb1Crb2^{F/+}$ cKO retinas (subretinal 2.10^{10} viral particles AAV2/9-CMV-*CRB2*; Fig. 2C and D).

We analyzed the photoreceptor morphology after expression of *CRB2* in both Müller glial cells and photoreceptors, which are the main affected cell types of *Crb2* cKO and $Crb1Crb2^{F/+}$ cKO (4,10,11). In the *Crb2* cKO, in areas expressing CRB2 (with GFP) cone (cone arrestin$^+$ cells) and rod (GFP$^+$ cone arrestin$^-$ cells) morphology was preserved (Fig. 3A). In areas expressing CRB2, a reduced number of ectopic photoreceptor synaptic terminals and gaps in the staining at the outer plexiform layer (PSD95) were found when compared with controls (Fig. 3B). The outer nuclear layer (ONL) thickness (*CRB2* 28 ± 2 versus *GFP* 18 ± 1 versus uninjected 22 ± 2 µm; Fig. 3C) and the number of cones was preserved in contrast to areas expressing GFP or uninjected (*CRB2* 11 ± 1 versus *GFP* 7 ± 1 versus not injected 6 ± 1 positive cells/100 µm; Fig. 3D). Similarly, $Crb1Crb2^{F/+}$ cKO retinas, in which only the inferior but not the superior region is affected, remained thicker in the inferior areas expressing CRB2 (*CRB2* 24 ± 2 versus *GFP* 16 ± 2 versus superior 42 ± 3 µm; Fig. 3E).

In contrast, targeting only Müller glial cells at P14 with *CRB2* did not improve b-wave retinal function compared to contralateral *GFP*-injected eyes in *Crb2* cKO (*CRB2* 86 ± 8 µV versus *GFP* 81 ± 16 µV; intravitreal 1.10^{10} viral particles AAV2/ShH10Y-CMV-*CRB2*; Supplementary Material, Fig. S2A) and $Crb1Crb2^{F/+}$ cKO (*CRB2* 238 ± 15 µV versus *GFP* 238 ± 29 µV; intravitreal 1.10^{10} viral particles ShH10Y-CMV-*CRB2*; Supplementary Material, Fig. S2B). Targeting of only photoreceptors at P14 with *CRB2* showed a slight decrease in b-wave retinal function which was not significant in *Crb2* cKO (*CRB2* 120 ± 9 µV versus *GFP* 150 ± 29 µV; subretinal 5.10^9 viral particles AAV9-GRK1-*CRB2*; Supplementary Material, Fig. S2C) and $Crb1Crb2^{F/+}$ cKO (*CRB2* 112 ± 9 µV versus *GFP* 141 ± 32 µV; subretinal 5.10^9 viral particles AAV2/9-GRK1-*CRB2*; Supplementary Material, Fig. S2D).

In conclusion, targeting of both Müller glial cells and photoreceptors at P14 with *CRB2* showed amelioration of retinal function and morphology, whereas targeting exclusively to either Müller glial cells or photoreceptors did not.

Targeting of photoreceptors in newborn pups with *CRB2* did not improve retinal function

Crb2 cKO retinas display the first disorganization in the periphery of the retina at E18.5, which progress to a severe disorganization of the photoreceptor layer throughout the retina at P10 (10,11). We hypothesized that injection of *CRB2* vector at P14 may be too late to prevent the degeneration in photoreceptors as irreversible changes may have occurred by this time (Supplementary Material, Fig. S2C). To address this hypothesis and prevent further damage in newborn *Crb2* cKO retinas by subretinal injection, we used a systemic approach to express selectively CRB2 in the retinas of newborn pups. Previous studies have shown that

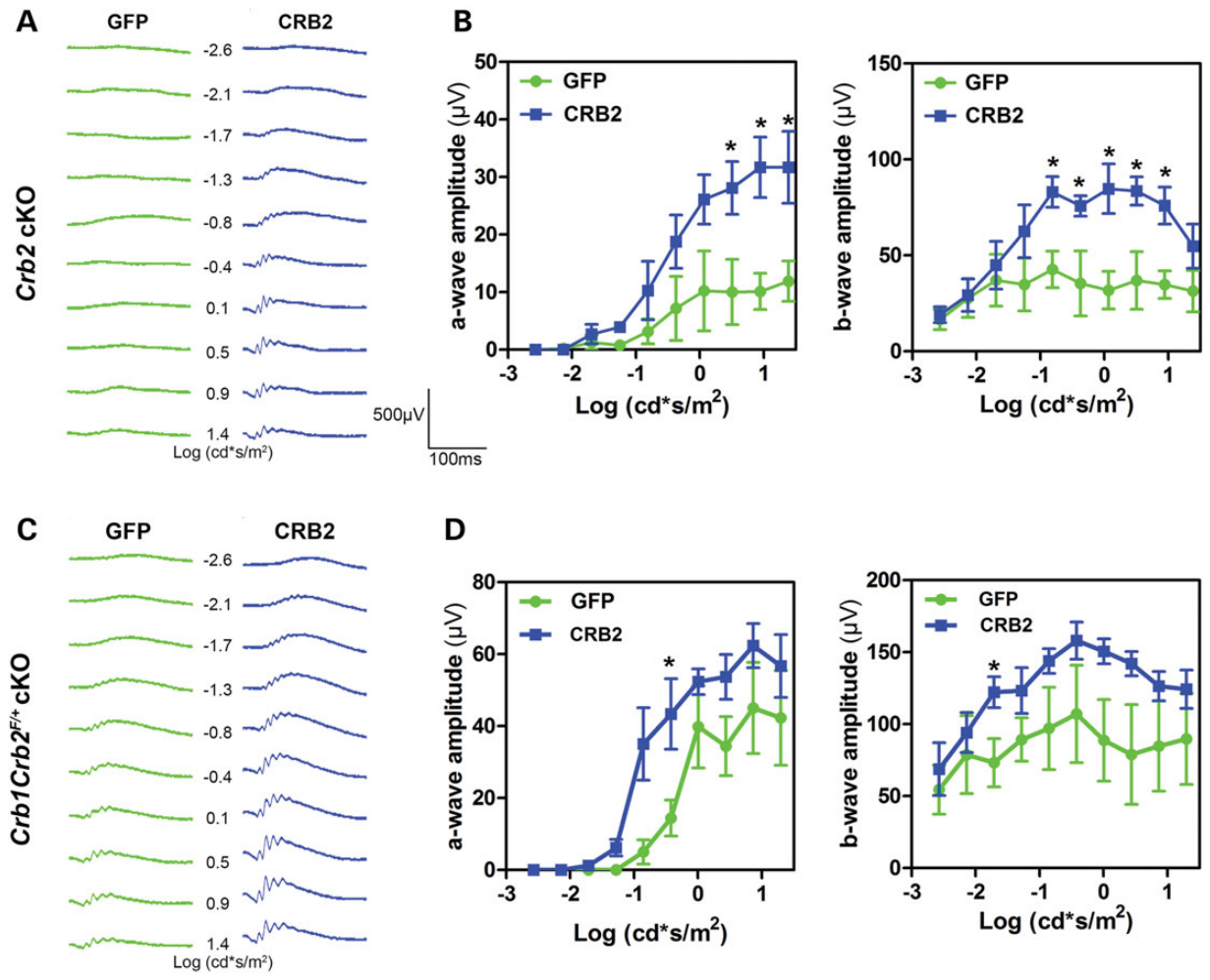

Figure 2. Improvement of retinal function by targeting both Müller glial cells and photoreceptors with human *CRB2* in two *CRB1*-RP mouse models. Scotopic single-flash ERG responses from the same representative animal (**A** and **C**) and mean ± SEM of all animals for A-wave (left panels) and B-waves (right panels) amplitudes (**B** and **C**) under scotopic conditions were presented. Improvement of retinal function was observed in AAV2/9-CMV-*CRB2* subretinally injected eyes compared to contralateral AAV2/9-CMV-*GFP* subretinally injected eyes, which target Müller glial cells and photoreceptors (and retinal pigment epithelium) with 2.10^{10} genome copies in 3 M-old *Crb2* cKO retinas ($n = 5$; A and B) and 4 M-old *Crb1Crb2*$^{F/+}$ cKO ($n = 7$; C and **D**). *$P < 0.05$.

systemic injections of AAV9 via the intravenous route (tail vein or facial vein) or intra-arterial route (left ventricular cavity) in newborn pups reach the retina (23,24), we tested and compared other systemic laboratory techniques: retro-orbital and intraperitoneal injections of AAV9 (Supplementary Material, Fig. S3). Systemic intraperitoneal injection of AAV9-CMV-*GFP* at P5 lead after three weeks to GFP expression just above detection level as observed by scanning laser ophthalmoscopy (SLO) and transverse sections showed many GFP positive ganglion, amacrine, bipolar and Müller glial cells (Supplementary Material, Fig. S3A). In contrast, systemic retro-orbital injections of AAV9-CMV-*GFP* in littermate pups lead to efficient transduction of the retina visible on SLO and transverse sections after three weeks (Supplementary Material, Fig. S3B–D). In addition to the transduced ganglion, amacrine, bipolar, horizontal, Müller glial and few retinal pigment epithelium cells, the ipsilateral (injected) side showed more retinal pigment epithelium, choroid and sclera cells transduced than the contralateral (transduced via the blood stream only) side (Supplementary Material, Fig. S3B and C). Retinal function assessed in eyes retro-orbitally injected with AAV9-CMV-*GFP* showed a reduced b-wave amplitude in the ipsilateral side compared to the contralateral side and was associated with reduced ONL thickness (Supplementary Material, Fig. S3E and F). This finding is much likely due to damage by the surgical procedure in neonates rather than caused by AAV expression or immune responses to the vector. We tested two human photoreceptor specific promoters, GRK1 (rods and cones) and rhodopsin (RHO, rods only), which were previously tested in adult animals via subretinal injection (4,25). Via the retro-orbital route (Supplementary Material, Fig. S3G and H), SLO showed no or low detectable GFP expression with GRK1 and RHO promoters (white arrowheads, Supplementary Material, Fig. S3G and H). Furthermore, retro-orbital injection with the ubiquitous CMV promoter lead to high transduction of other tissues such as liver, skeletal muscles, heart and brain tissues, whereas the use of the GRK1 promoter restrained GFP expression to only few cells in the liver (Supplementary Material, Fig. S4A–D). Retro-orbital injection lead to GFP expression in astrocytes and few neurons in the visual cortex (Supplementary Material, Fig. S4D–F). Systemic retro-orbital injections showed good efficiency to transduce retinal cells and GRK1 promoters lead to specific expression in photoreceptors.

We performed systemic retro-orbital injection at P3 with $1–2.10^{11}$ AAV9-GRK1-*CRB2* viral particles and used only the

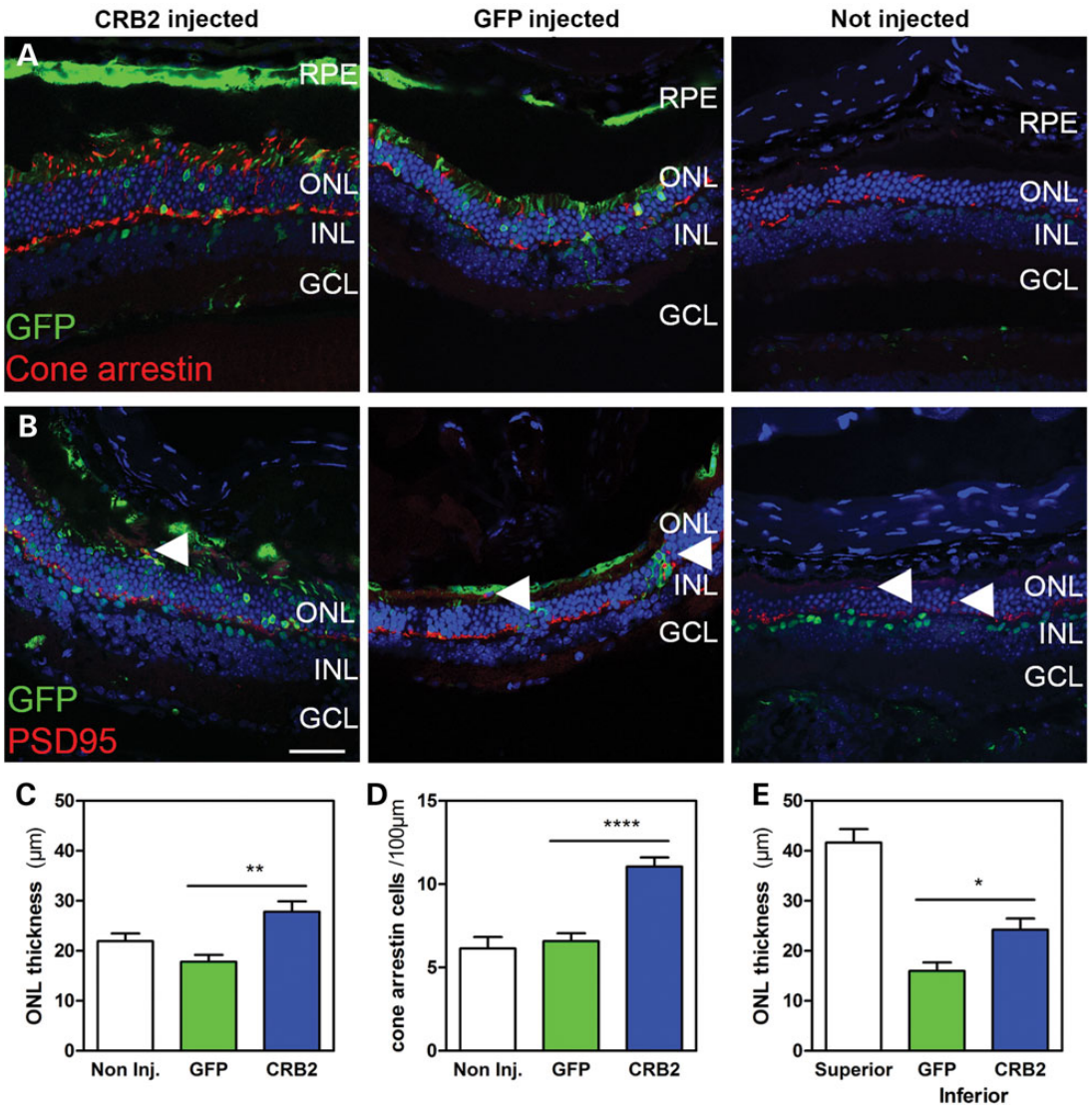

Figure 3. CRB2 expression in Müller glial cells and photoreceptors improved photoreceptor layer morphology. Increased number of cone arrestin positive (cones) cells (**A** and **D**), decreased number of ectopic PSD95 (synapses) stainings (white arrowheads in **B**) and thicker ONL (**C**) were found in CRB2 (+1/10 GFP) injected areas than GFP or not injected areas in 3 M-old *Crb2* cKO retinas ($n = 5$) injected subretinally with 2.10^{10} genome copies of AAV2/9-CMV-*CRB2* subretinally. The ONL in the inferior retina, which is only affected in *Crb1Crb2*$^{F/+}$ cKO was thicker in *CRB2* (spiked with 2.10^{9} gc of *GFP*) injected areas than *GFP*-injected areas in 4 M-old *Crb1Crb2*$^{F/+}$ cKO ($n = 5$) injected subretinally with 2.10^{10} genome copies of AAV2/9-CMV-*CRB2* subretinally (**E**). GCL, ganglion cell layer; INL, inner nuclear layer; Not Inj, Not injected; ONL, outer nuclear layer; PSD95, Post synaptic density 95 kDa; RPE, retinal pigment epithelium. Data are presented as mean ± SEM. *$P < 0.05$, **$P < 0.01$ and ****$P < 0.0001$. Scale bar: 50 µm.

contralateral side to measure retinal function at 3 M in *Crb2* cKO eyes. We did not find any improvement of the retinal function (Supplementary Material, Fig. S2E) compared to AAV9-GRK1-*GFP* eyes for the a-wave (*CRB2* 59 ± 16 µV versus *GFP* 66 ± 23 µV) or b-wave (*CRB2* 164 ± 39 µV versus *GFP* 185 ± 28 µV) at 3 M of age.

In summary, early targeting of only photoreceptors by *CRB2* was not sufficient to prevent retinal degeneration.

Expression of human CRB1 protein in the eye leads to reduced retinal function

Similarly to *CRB2*, we performed injection with *CRB1* vectors in either Müller glial cells or photoreceptors or both in order to prevent retinal degeneration in *Crb1Crb2*$^{F/+}$ cKO mice (Fig. 4). Previously, we showed that human CRB1 expressed at the subapical region after subretinal injection of AAV9-minCMV-*hCRB1* and AAV9-GRK1-*hCRB1* (22). Here, we tested intravitreal injection of ShH10Y-minCMV-*hCRB1*. Human CRB1 protein was found only just at detectable levels at the subapical region from Müller glial cells in *Crb1*$^{-/-}$ retinas (white arrowheads, Supplementary Material, Fig. S5).

When targeting both Müller glial cells and photoreceptors (and retinal pigment epithelium) with *CRB1*, maximal responses for scotopic a-wave (*CRB1* 22 ± 10 µV versus *GFP* 48 ± 4 µV) and scotopic b-wave (*CRB1* 68 ± 6 µV versus *GFP* 102 ± 20 µV) were reduced in all eyes whereas photopic b-waves (*CRB1* 26 ± 8 µV versus *GFP* 27 ± 9 µV) were not different (subretinal 1.10^{10} viral particles AAV9-minCMV-*CRB1*; Fig. 4A). Surprisingly, using the intravitreal route to express CRB1 in Müller glial cells (intravitreal 5.10^{9} viral particles ShH10Y-minCMV-*CRB1*; Fig. 4B), drastic

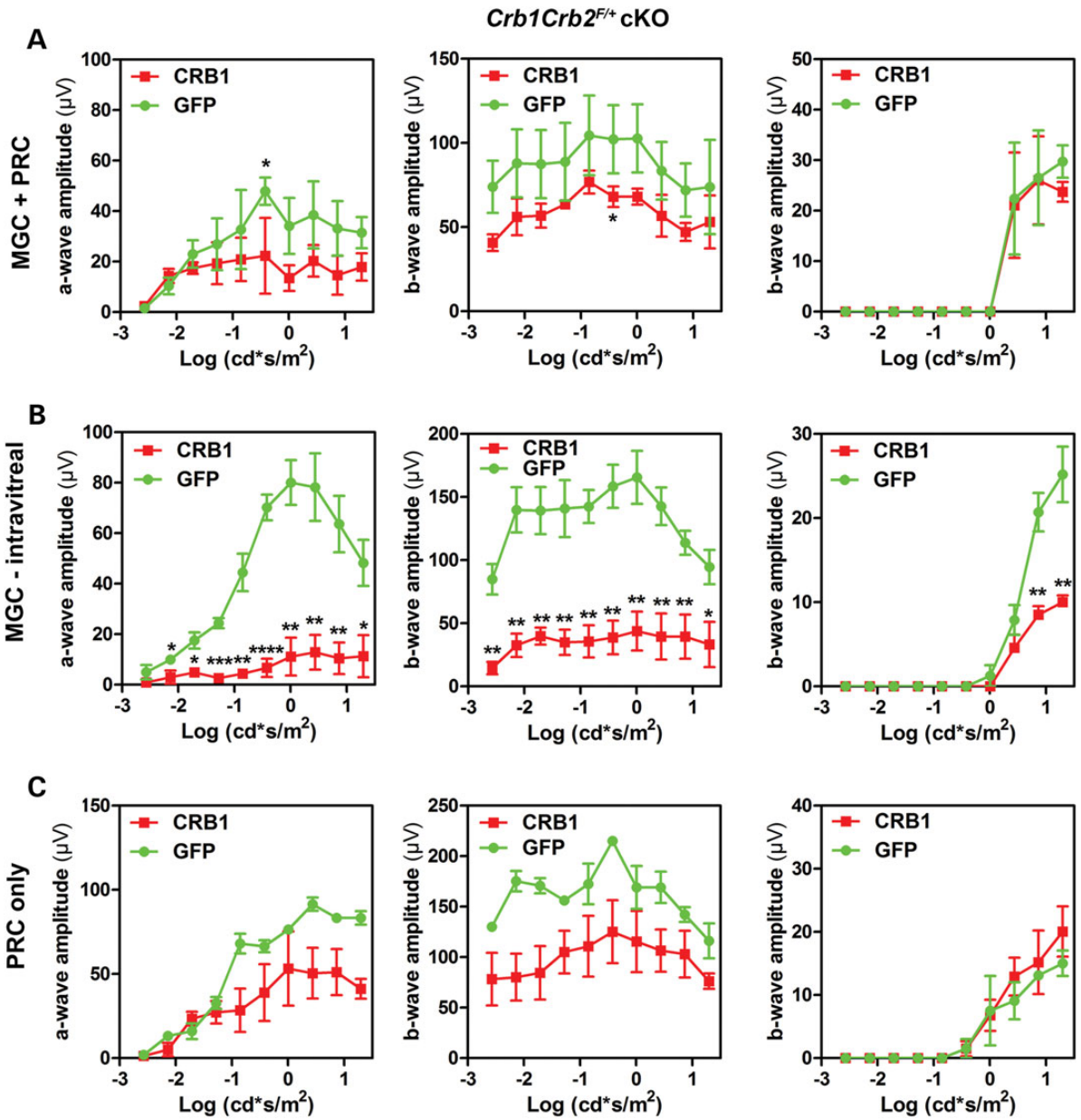

Figure 4. Reduction of retinal function upon injection of human *CRB1* in the eye. Decrease of a-wave (left panels) and b-waves (middle panels) under scotopic conditions and b-waves under photopic conditions was observed in eyes injected subretinally with 10^{10} genome copies of AAV2/9-minCMV-*CRB1* targeting Müller glial, photoreceptor and retinal pigment epithelium ($n = 5$; **A**), intravitreally with 5.10^{9} genome copies of AAV2/ShH10Y-minCMV-*CRB1* targeting Müller glial cells and cells in the inner, ganglion layers, ciliary body and iris ($n = 4$; **B**) or retro-orbitally with $1–2.10^{11}$ genome copies of AAV2/9-GRK1-*CRB1* targeting only photoreceptors ($n = 3–4$; **C**) in 5 M-old *Crb1Crb2*$^{F/+}$ cKO. MGC, Müller glial cells; PRC, photoreceptor cells. Data are presented as mean ± SEM. $^{*}P < 0.05$ and $^{**}P < 0.01$.

reduction in retinal function in all eyes was found for scotopic a-wave (*CRB1* 13 ± 7 µV versus *GFP* 78 ± 13 µV), scotopic b-wave (*CRB1* 44 ± 15 µV versus *GFP* 166 ± 21 µV) and photopic b-wave (*CRB1* 10 ± 1 µV versus *GFP* 25 ± 3 µV). Systemic retro-orbital injection with AAV9-GRK1-*CRB1* at P3 in *Crb1Crb2*$^{F/+}$ cKO induced decrease of the retinal function (retro-orbital contralateral eyes $1–2.10^{11}$ viral particles AAV9-GRK1-*CRB1*; Fig. 4C) compared to contralateral *GFP*-injected eyes for the scotopic a-wave (*CRB1* 51 ± 14 µV versus *GFP* 83 ± 2 µV) or scotopic b-wave (*CRB1* 111 ± 30 µV versus *GFP* 172 ± 12 µV) but not for the photopic b-wave (*CRB1* 15 ± 5 µV versus *GFP* 13 ± 1 µV).

After 4.5 M post-intravitreal injection of *CRB1* vector, the eyes were found to be smaller and degenerative compared to contralateral *GFP* eyes (Fig. 5A and B). Intravitreal injection of *GFP* revealed that the transduced eye tissues were the retina, the ciliary body and the iris but not the lens or the cornea (Fig. 5C–F). CRB1 protein was only detected in few cells and the retina, the ciliary body and the iris showed abnormal morphologies (Fig. 5G–J). However, the retina, the ciliary body and the iris were highly affected (Fig. 5G–J) compared to *GFP* (Fig. 5C–F). Especially, the double epithelium of the ciliary body and iris and the ciliary processes disappeared (Fig. 5I and J). Multivariate analysis of variance (MANOVA) was calculated to compare GFP versus CRB1 injected eyes for seven different measurements relating to eye morphology. The overall effect of Wilks′ Lambda was significant ($F(6,1) = 2382.032$, $P = 0.016$) meaning that there is a

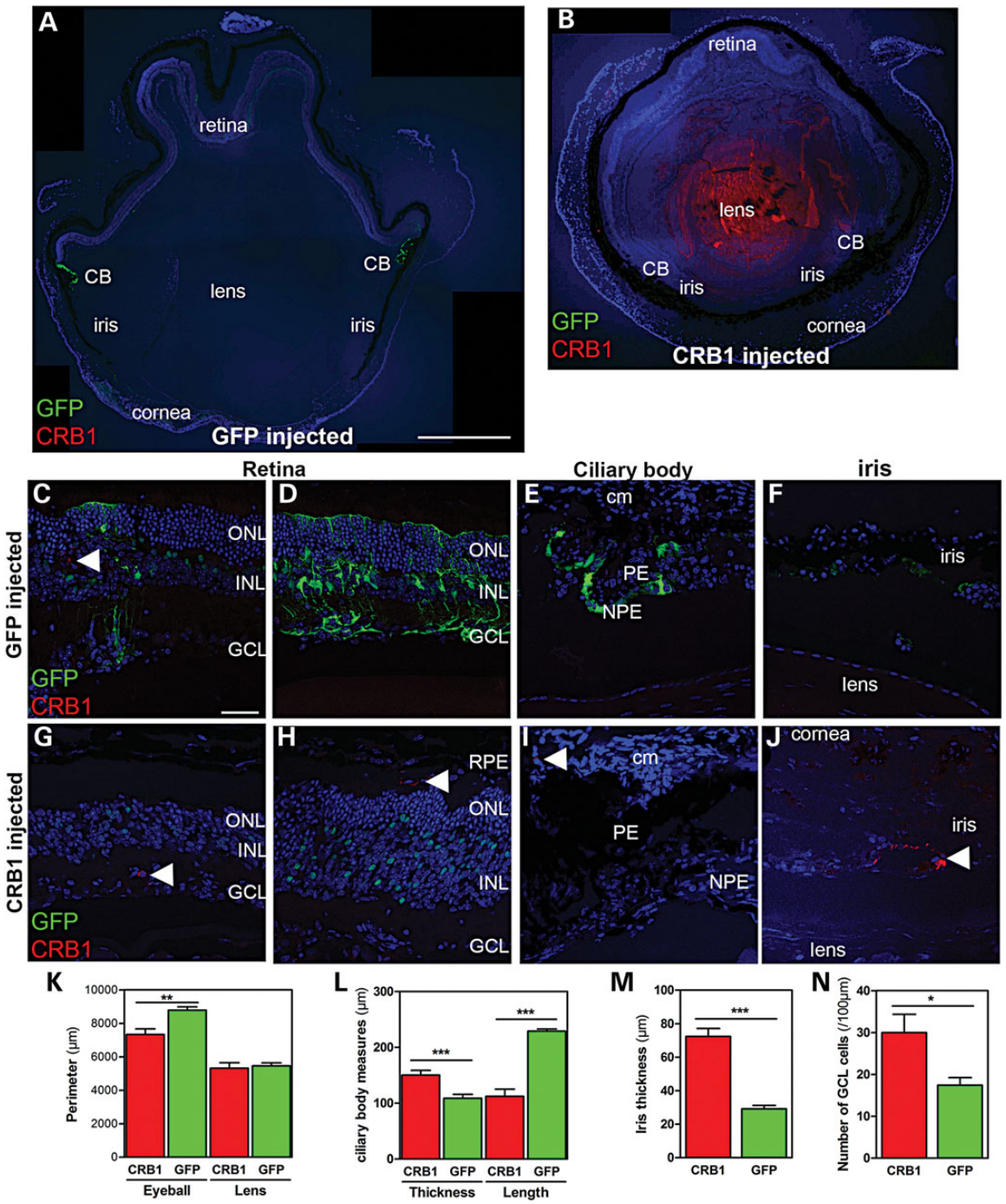

Figure 5. Massive disorganization of the ciliary body, iris and retina upon intravitreal injection of human *CRB1*. After 4.5 M post-intravitreal injection of 5.10^9 genome copies of AAV2/ShH10Y-minCMV-*CRB1* into *Crb1Crb2*$^{F/+}$ cKO retinas (**B**) eyes were reduced in size compared to contralateral *GFP*-injected eyes, which showed the highest transduction in the ciliary body (**A**). Inferior areas of the retina, which display the retinal phenotype (associated with red dotty staining due to degeneration, white arrowhead, **C**), and non-affected areas (**D**) showed that mainly Müller glial cells are transduced in *GFP*-injected eyes. The non-pigmented ciliary epithelium of the ciliary body is highly transduced (**E**) and the iris epithelium at lower levels (**F**). In *CRB1*-injected eyes, the ONL was affected with almost complete lack of photoreceptors (**G**) to at least reduced number (**H**) in wavy retinas and few CRB1 positive cells were found throughout the retina (white arrowheads, G–I). The typical structure of the ciliary processes formed by the two epithelia (I) and the epithelium of the iris (**J**) were totally disorganized. Despite few positive cells, CRB1 staining was found only in few cells of the iris (white arrowhead, J). The perimeter of the *CRB1*-injected eyes was reduced but the lens showed similar perimeter length as *GFP*-injected eyes (**K**). The length of the ciliary body (**L**) was reduced whereas the thickness of the ciliary body (L) or iris (**M**) was increased in *CRB1*-injected eyes compared to GFP-injected eyes. The number of cells in the ganglion cell layer was increased in *CRB1*-injected eyes (**N**). CB, ciliary body; cm, ciliary muscles; GCL, ganglion cell layer; INL, inner nuclear layer; NPE, non-pigmented ciliary epithelium; ONL, outer nuclear layer; PE, pigmented ciliary epithelium; RPE, retinal pigment epithelium. Data are presented as mean ± SEM. *$P < 0.05$, **$P < 0.01$ and ***$P < 0.001$. Scale bar: 500 µm (A and B), 50 µm (C–J).

Table 1. Eye measurements of the eye structures upon intravitreal injection of human *CRB1*

	CRB1 (μm)	GFP (μm)	*F*	P-value	Partial Eta^2
Eyeball perimeter	7341 ± 333	8788 ± 199	13.847	0.010	0.698
Lens perimeter	5317 ± 329	5462 ± 175	0.150	0.721	0.024
Ciliary body thickness	150 ± 9	109 ± 7	14.120	0.009	0.702
Iris thickness	72 ± 5	29 ± 2	71.505	0.000	0.923
Ciliary body length	112 ± 13	229 ± 4	78.023	0.000	0.929
Retina length	4634 ± 466	4867 ± 226	0.202	0.699	0.033
Cornea thickness	157 ± 13	115 ± 3	9.017	0.024	0.600

significant difference between the two groups with respect to the seven eye-measures. Subsequent univariate tests for each measure were conducted and reported in Table 1. Measurements showed that the eyeball perimeter but not the lens perimeter was reduced significantly compared to *GFP* (Fig. 5K, Table 1). The ciliary body thickness and iris thickness were increased and the ciliary body length was decreased significantly compared to *GFP* eyes (Fig. 5L and M, Table 1). The lamination of the retina was affected associated with reduced number of photoreceptors and increased number of cells in the ganglion cell layer (*CRB1* 30 ± 4 versus *GFP* 17 ± 2 cells/100 μm; Fig. 5N) compared to *GFP*-injected eyes. However, the length of the retina was not different than GFP-injected eyes (Table 1). The thickness of the cornea was significantly increased probably due to a secondary effect, as it was not directly transduced by the intravitreal injection. This was not as highly significant as other measurements but the effect size, calculated as Partial Eta^2, is comparable (Fig. 5A and B, Table 1).

In summary, CRB1 expression in the eye negatively affected the morphology of the retina, ciliary body and iris and reduced the retinal function.

Infiltration of immune cells and early expression of CRB1 or CRB2 in ciliary body and iris epithelia

The drastic effect of human *CRB1* injection intravitreally on ciliary body, iris and retina could be explained by an immune reaction to human CRB1 at the cell surface in naïve *Crb1* mice or a deleterious effect of CRB1 protein itself or both. We investigated the first hypothesis using markers for immune cells. After 4.5 M post-intravitreal injection of *CRB1* vector, the number of infiltrated T-cells (CD3) were drastically increased compared to contralateral GFP-injected eyes in the remaining ciliary body and iris structures (*CRB1* 94 ± 5 versus *GFP* 22 ± 5 cells; Fig. 6A–C) and in the retina (Fig. 6D and E), but not in the lens or cornea. Similarly, an increased number of myeloid cells (macrophages and microglial cells; CD11b) were found in the ciliary body (*CRB1* 8.1 ± 1.0 versus *GFP* 1.5 ± 0.3 cells; Fig. 6F–H) and retina (Fig. 6I and J). In conclusion, the tissues lacking endogenous mouse Crb1 that expressed human CRB1 showed increased infiltration of CD3 positive T cells and CD11b positive myeloid cells.

Via the intravitreal route, *CRB1*-injected eyes, but not *CRB2*, showed reduced retinal function (Fig. 4B and Supplementary Material, Fig. S2A and B). We hypothesized that early expression of CRB1, but not of CRB2, lead to disorganization of the ciliary body and iris epithelia. Therefore, we investigated mouse endogenous Crb1 and Crb2 expression and human CRB1 and CRB2 expression and their effects short term after intravitreal injection in these tissues. Three weeks after intravitreal injection of ShH10Y-*GFP* in WT retinas, GFP was detected in ciliary body and iris epithelia (Fig. 7A–D) similarly to 4.5 months after injection (Fig. 5). GFP was strongly expressed in the non-pigmented ciliary epithelium and at lower levels in the iris epithelium. No detectable mouse Crb1 and Crb2 proteins were found in wild-type ciliary body, iris, cornea or lens (Fig. 7A–D) in contrast to retina (Fig. 1A and Supplementary Material, Fig. S5A). However, strong expression of human CRB2 and CRB1 were detected three weeks after intravitreal injection of ShH10Y-CMV-*CRB2* in *Crb2* cKO and ShH10Y-minCMV-*CRB1* in *Crb1*$^{-/-}$, respectively (Fig. 7E and F). Already three weeks after AAV delivery, *CRB1*-transduced ciliary body appeared more elongated and slightly disorganized compared to the *CRB2*-transduced ciliary body. This might indicate that CRB1 protein itself display deleterious effects in epithelial cells.

In summary, endogenous Crb1 and Crb2 proteins were below detection level in the wild-type ciliary body, and ectopic expression of human CRB1, but not CRB2, transmembrane protein in ciliary bodies of *Crb1*$^{-/-}$ retinas caused invasion of immune cells and tissue degeneration.

Expression of CRB1 or CRB2 did not alter retinal function in healthy retinas

In preparation for the use of our *CRB* vectors for clinical applications, we performed pre-clinical studies in mouse retinas expressing normal levels of endogenous Crb1 and Crb2 (*Crb2*$^{F/F}$ mice not expressing *Cre*) to study the potential adverse effect of the *CRB2* and *CRB1* vectors and measured the retinal function. No difference on scotopic b-wave amplitude was observed via intravitreal injection of ShH10Y-CMV-*CRB2* (*CRB2* 144 ± 34 μV versus *GFP* 134 ± 38 μV; 1.10^{10} viral particles) or intravitreal injection of ShH10Y-minCMV-*CRB1* (*CRB1* 221 ± 14 μV versus *GFP* 223 ± 45 μV; 5.10^{9} viral particles) compared to contralateral *GFP*-injected eyes or non-injected eyes (Supplementary Material, Fig. S6A–C).

We conclude that recombinant human CRB1 or CRB2 expression had no adverse side effects on the retinal function in mouse retinas expressing endogenous Crb1 and Crb2.

CRB proteins localization in the inner segments of human photoreceptors

We found unexpected expression of human CRB2 at the tip of mouse photoreceptor inner segments only when *CRB2* was specifically targeted to photoreceptors using the specific GRK1 promoter (Fig. 1D). Previously we showed by immunohistochemistry a similar pattern of expression for CRB2 in the inner segments of human retina (4). Therefore, we examined our immuno-electron microscopy for localization of CRB proteins in the inner segments of human photoreceptors.

A CRB1 antibody raised against the intracellular domain recognized potentially two CRB1 protein isoforms in human donor retinas (Supplementary Material, Fig. S1A; 4). Immuno-electron microscopy with this antibody showed specific staining in vesicle structures in the myoid region of the inner segment of rods and cones (black arrowheads; Fig. 8A and C). The antibody raised against the extracellular epitope of CRB1 recognizes all three CRB1 protein isoforms (4). Immuno-electron microscopy with this antibody showed extended staining in the cytoplasmic

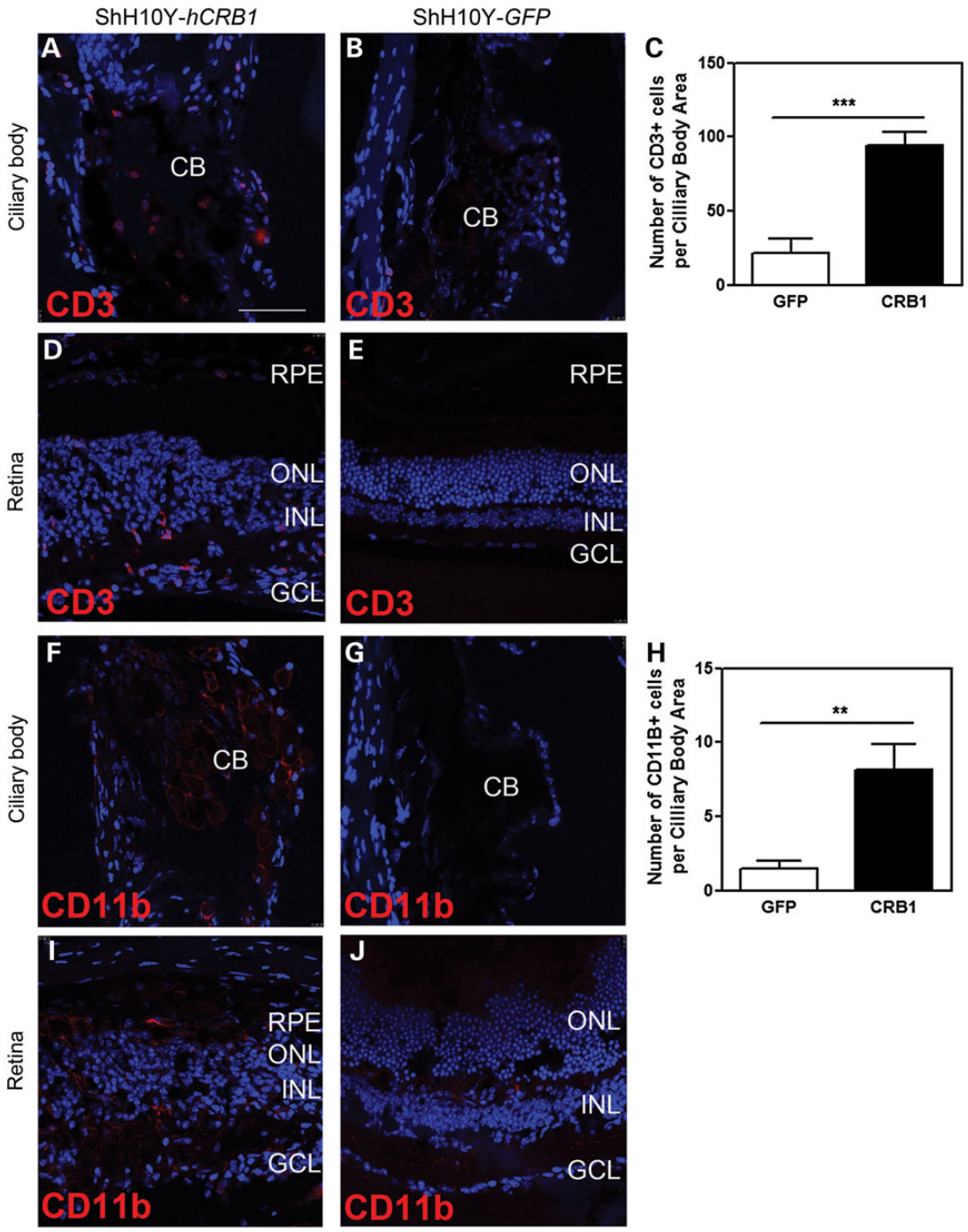

Figure 6. Intravitreal injection of human *CRB1* in retinas lacking endogenous Crb1 induces invasion of immune cells in tissues expressing CRB1. After 4.5 M post-intravitreal injection with 10^9 genome copies of AAV2/ShH10Y-minCMV-*CRB1*, *Crb1Crb2*$^{F/+}$ cKO eyes showed an increased number of CD3 positive cells (T-cells) in the ciliary body (**A**) and retina (**D**) compared to contralateral *GFP*-injected ciliary body (**B**) and retina (**E**). Quantification of CD3 positive cells in the ciliary body was significantly higher in *CRB1*-injected eyes (**C**). *CRB1*-injected eyes exhibited an increase in CD11b expressing cells (myeloid cells) in both the ciliary body (**F**) and retina (**I**) compared to the contralateral *GFP*-injected ciliary body (**G**) and retina (**J**). Quantification of CD11b positive cells in the ciliary body was significantly higher in *CRB1*-injected eyes (**H**). CB, ciliary body; GCL, ganglion cell layer; INL, inner nuclear layer; ONL, outer nuclear layer. Data are presented as mean ± SEM. $^{**}P < 0.01$ and $^{***}P < 0.001$. Scale bar: 50 µm.

compartment between the mitochondria in the myoid region of the inner segment of rods and cones (black arrowheads; Fig. 8B and D). Dense CRB2 staining was exclusively found in between mitochondria in the ellipsoid region of the inner segments (black arrowheads; Fig. 8E), presumably in the striated ciliary rootlets. Strong and localized CRB3A staining was found in the ellipsoid region in the vicinity of the basal body (black arrowheads; Fig. 8F). In addition, we reported previously that CRB3A was found also in the outer plexiform layer and in blood vessels by immunohistochemistry (4). Immuno-electron microscopy in the outer

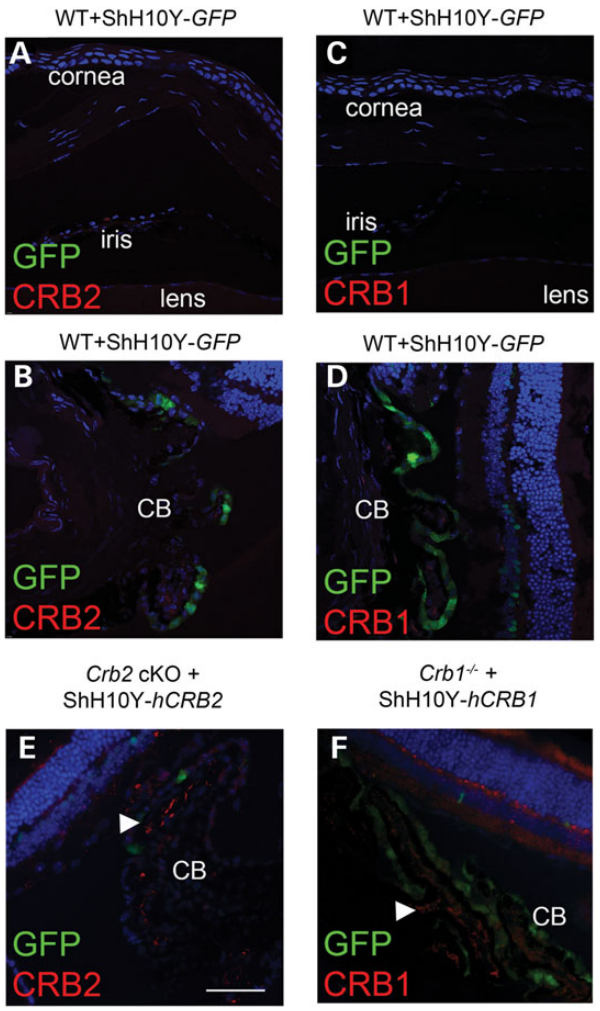

Figure 7. Expression of CRB1 and CRB2 in the ciliary body and iris epithelia after intravitreal injections. No endogenous mouse Crb2 or Crb1 expression was detected in the cornea, the edge of the iris, lens or ciliary body tissues (**A–D**) in wild-type retinas. A strong tropism for the ciliary body (non-pigmented epithelium) was observed after 3 weeks post-injection of 10^{10} genome copies of AAV2/ShH10Y-CMV or minCMV-*GFP* virus (B and D) and not for the iris, the lens and the cornea (A and C). After three weeks post-injection intravitreally in *Crb2* cKO retinas of 2.10^{10} genome copies of ShH10Y-CMV-*CRB2* (**E**), strong human CRB2 protein was detected in the ciliary body. After three weeks post-intravitreal injection of 5.10^{9} genome copies of ShH10Y-minCMV-*hCRB1* (**F**) in *Crb1*$^{-/-}$ retinas, human CRB1 protein was highly expressed in the ciliary body. CB, ciliary body. $n = 2–4$/viral vector. Scale bar: 50 µm.

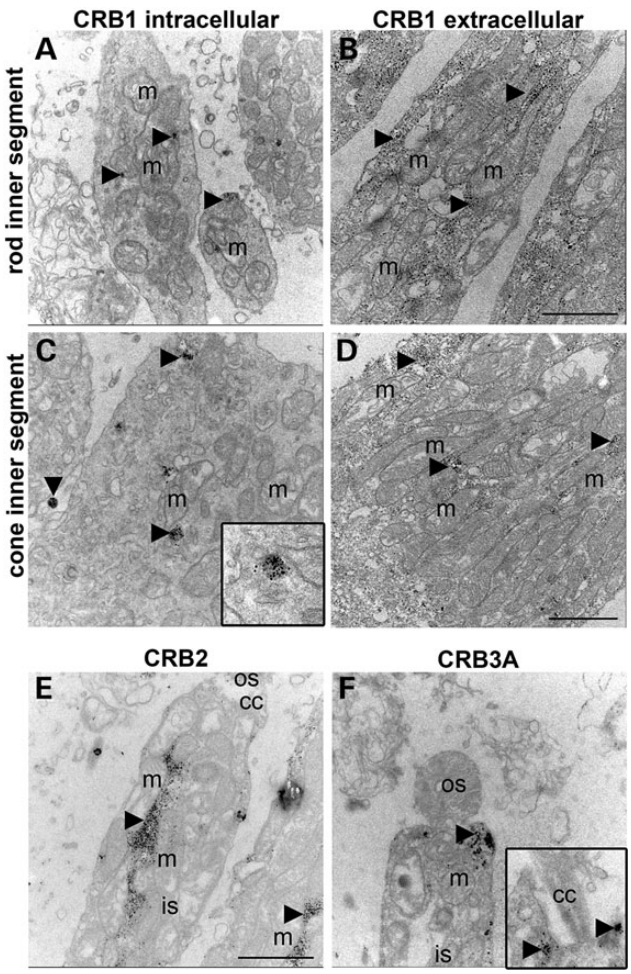

Figure 8. Ultrastructural localization of CRB1, CRB2 and CRB3A in the inner segments of human retina. Immuno-electron microscopy against the intracellular domain of CRB1 (two isoforms) revealed that CRB1 is located in membrane vesicles in the inner segment of rods (**A**) and cones (**C**) whereas immuno-electron microscopy against the extracellular domain (three isoforms) showed CRB1 expression in between the mitochondria and in membrane vesicles of the inner segment of rods (**B**) and cones (**D**). CRB2 was found only in the myeloid of the inner segment between mitochondria (**E**). CRB3A is located and concentrated in the vicinity of the connecting cilium cells (**F**). cc, connecting cilium; is, inner segment; m, mitochondria; os, outer segment. Scale bar: 1 µm (A–F).

plexiform layer revealed CRB3A staining in the dendrites of the rod bipolar cells only in rod synaptic terminals and in the pericyte cells aligning the blood vessels (Supplementary Material, Fig. S7A and B).

In summary, the three CRB members showed different distribution patterns along the inner segments, with at the tip region CRB3A, in the ellipsoid region CRB2 and in the myoid region CRB1.

Discussion

In this study, we show that (a) human *CRB2* cDNA can be efficiently packaged in AAV vectors and generates efficient CRB2 expression after injection *in vivo*. (b) After AAV gene delivery, human CRB2 was expressed primarily at the subapical region when targeted to photoreceptors and Müller glial cells, or to only Müller glial cells, and mainly at the tip of the photoreceptor segments when targeted only to photoreceptors. (c) Only targeting of both Müller glial cells and photoreceptors with *CRB2* but not in one unique cell type lead to improved retinal activity and morphology in mid-onset progression of *CRB1*-RP mouse models. (d) Targeting only photoreceptors with *CRB2* in early onset of degeneration *CRB1*-RP mouse retinas did not improve retinal activity. (e) Expression of CRB1 in *Crb1Crb2*$^{F/+}$ cKO via the intravitreal, subretinal and retro-orbital routes impaired retinal function. (f) Ectopic expression of human CRB1 transmembrane protein in *Crb1* knock-out ciliary epithelium causes tissue degeneration and invasion of immune cells, whereas ectopic CRB2 transmembrane protein expression in *Crb2* cKO ciliary epithelium does not cause tissue degeneration. (g) Overexpression of human CRB1 and CRB2 in retinas expressing endogenous levels of mouse Crb1 and Crb2 did not alter retinal activity or morphology. (h)

Besides the subapical region, human CRB1, CRB2 and CRB3A have unique patterns of localization within photoreceptor inner segments. In conclusion, we showed the first extensive pre-clinical efficacy studies for CRB1-related eye disorders using *CRB2* vectors.

Interestingly, we found a different pattern of human CRB2 expression at the subapical region in mouse retinas when CRB2 was expressed only in photoreceptors (using the GRK1 promoter) than in both Müller glial cells and photoreceptors (using the CMV promoter). Expression of CRB2 in mouse photoreceptors was mainly at the tip of the inner segments and at lower amounts at the subapical region. When CRB2 is targeted to both Müller glial cells and photoreceptors, CRB2 was mainly found at the subapical region and at lower amounts in the inner segments. Improvements in retinal function are found only when CRB2 is targeted to both Müller glial cells and photoreceptors in the two *CRB1*-RP mouse models. These results suggest that the primary function of CRB2 is at the subapical region where it is involved in Müller glial cell-photoreceptor interactions. Others have demonstrated that direct intercellular interaction of the extracellular domains of zebrafish Crb2 play an essential role for photoreceptor cell-cell adhesion and function (26). Here, we hypothesize that in mammals similar intercellular interactions may occur between the extracellular domains of human CRB2 from Müller glial cells and from photoreceptors. This direct CRB2 interaction might localize and maintain CRB2 at the subapical region and allow the formation of adherens junctions between the two cell types. In contrast, when CRB2 is targeted only to photoreceptors, human CRB2 could not be maintained at the subapical region or only poorly via photoreceptor–photoreceptor interaction, and become internalized in the photoreceptor inner segments. In this study, we showed the first intercellular mechanisms of CRB proteins in mammals. Future investigations on the functional role of CRB1 and CRB2 in the different cell types and their extracellular domains will allow to fully understand their functions at the subapical region in mammalian retinas.

The expression of human CRB2 in murine photoreceptors remarkably resemble the localization of CRB2 observed in human retinas in the inner segment ellipsoid. We hypothesize that human CRB2 may have an additional function in the ellipsoid such as in determining the photoreceptor segment length. We and others have shown that Crb2 in mice and zebrafish was involved in determining the cone outer segment length and rod inner and outer segments (10,27). CRB1 and CRB3A were found in the inner segments at different locations. Further investigations on the putative role(s) of human CRB1, CRB2 and CRB3 in the photoreceptor inner segments in mouse retinas might indicate their functions and relevance for human physiology.

Independent of the cell type(s) targeted, the AAV serotype or the route of administration used, expression of human CRB1 protein leads to reduced retinal electrophysiologic responses in *Crb1Crb2*$^{F/+}$ cKO. The most severe adverse effects were observed in eyes injected intravitreally. We show here that AAV-ShH10Y particles efficiently transduce the epithelium of ciliary body and iris in addition to the Müller glial cells in the mouse retina. CRB1 overexpression in the epithelium of ciliary body and iris of *Crb1* knockout retinas had drastic effects on the lamination and physiology of the epithelium. The major functions of the ciliary body in the eye is the secretion of the components of the vitreous such as aqueous humor and glycoproteins, the maintenance of the intraocular pressure and the shape of the lens through the ciliary muscles (28). Therefore, the drastic decrease of the eyeball size might be due to the destruction of the ciliary body processes and epithelium leading to defects in intraocular pressure and an abnormal concentration of vitreous components. As the lens shape and diameter were not affected by CRB1 expression and the ciliary muscles were conserved, we presume that this deleterious effect was restricted to junctional complexes in the ciliary body.

Fortunately, CRB2 transduced into the ciliary body and iris of *Crb1Crb2*$^{F/+}$ cKO and *Crb2* cKO retinas does not cause side effects as observed with CRB1. CRB2 and CRB1 are structurally very similar in their extracellular, transmembrane and intracellular domains. Especially the 37 amino acid C-termini, which contains at least two protein-recognition motifs, are highly conserved. Differences in amino acid composition in protein-recognition motifs of CRB proteins may affect CRB protein complex stability and composition, allowing a larger window of normal CRB2 compared to CRB1 expression. For example overexpression of CRB1 may severely disturb apical polarity of epithelia, whereas variations in CRB2 levels are more tolerable. However, next to similar functions for CRB2 and CRB1, we cannot exclude unique functions for each of the proteins. Further investigations using CRB1/CRB2 chimeric proteins may help to understand which domains and amino acids lead to adverse side effects and might be prevented by direct-site directed mutagenesis of CRB1. We showed that in addition a severe infiltration of immune cells are present in all tissues that express CRB1. The *Crb1* mice are naïve for any CRB1 protein and the expression of human CRB1 at the cellular surface in *Crb1* KO background mice induced an immune reaction. Normally, the healthy eye is a partially-immune privileged site, physically via its retinal blood barrier and its natural immuno-suppression ability to maintain transparent tissues required for vision. However, the retinal blood barriers are compromised in *Crb1* KO and *Crb2* cKO retinas (6,10). Over the last several years, extensive studies on the potential immunogenicity of AAV and its relative transgene revealed no or little production of antibodies upon injection in the retina in humans and animal models (28). But the overexpression of transmembrane protein CRB1 especially in eye tissues in tight relation with blood vessels such as the ciliary body might expose the extracellular domains of human CRB1 as an antigen to the immune system in the *Crb1* mouse. Mice that express endogenous levels of mouse Crb1 and Crb2 display no side effects after injection of human CRB1. The strongest adverse effects were observed following intravitreal administration, not by subretinal injection, which might be explained by differences in transduction of cell types and exposure to the immune system. Further investigations on a possible CRB1 immune reaction will be needed as it might be a crucial issue for the use of *CRB1* vectors in patients suffering from lack of CRB1 protein expression. Similar immune reactions might occur in patients completely lacking CRB1, but not in patients that timely express a CRB1 variant with amino acid substitutions. For example we showed previously that a C249W variant mouse Crb1 protein localized correctly at the subapical region (8), suggesting that some CRB1 variants might be expressed timely before the onset of development of the innate and adaptive immune systems. In contrast, as CRB2 is ubiquitously expressed in multiple vital organs such as lung, kidney and heart (29), as well as in photoreceptors and Müller glial cells, CRB2 protein is not likely to be immunogenic in humans and therefore is a preferred substitute for use in *CRB1*-related retinal dystrophy clinical trials.

In this study, we performed experiments in *CRB1*-RP mice at mid-stage of retinal degeneration to mimic the potential time window for the treatment of patients at the time of their disease state diagnosis. We also performed and described the use of two new and easy methods for systemic injection, intraperitoneal

and retro-orbital injections in early onset mouse models. We showed proof-of-principle studies using retro-orbital injection of *CRB1* and *CRB2* vectors under GRK1 promoters in early onset *CRB1*-RP mice with minimal retinal damage in the contralateral eye. Using either intraperitoneal or retro-orbital injections, additional rescue benefits might be obtained when targeting both Müller glial cells and photoreceptors before the onset of retinal degeneration in *CRB1*-RP mice. However, due to potential adverse effects in many vital organs, the ubiquitous CMV promoter could not be used to express CRB2. Thus, a Müller glial cell and photoreceptor specific promoter is required, which is challenging as the promoter has to be small (maximum of 0.6 kb) to carry *CRB2* cDNA and target rods, cones and Müller glial cells. A human *CRB1* promoter might be an excellent candidate but extensive investigations are needed to find the key transcriptional elements for Müller glial cells and photoreceptors and to be able to design a small promoter. Another option is the use of two independent AAV vectors targeting specifically either Müller glial cells or photoreceptors and injected at the same time. Whereas we showed here that AAV-GRK1-*GFP* vectors target only photoreceptors systemically, no small promoter targeting only Müller glial cells exists yet. Nevertheless, we and others have described large and Müller glial cell specific promoters (22,30,31) and analysis of the key elements in these promoters may allow the design of small promoters.

The intercellular mechanisms of CRB homomerization or heteromerization have to be considered in the design of *CRB* vectors for clinical applications. Further experiments in mice expressing specifically CRB1 or CRB2 in either photoreceptors or Müller glial cells will answer if human CRB2 forms only heteromers or could form heteromers with human CRB1. Here, we showed that endogenous mouse Crb1 expressed in Müller glial cells did not maintain human CRB2 at the subapical region when targeted only to photoreceptors. However, in human CRB1 retinopathy context, low levels of endogenous CRB2 are expressed in human photoreceptors and targeting photoreceptors specifically with recombinant CRB2 to elevate endogenous levels might be sufficient to prevent retinal degeneration as CRB2 proteins are well expressed at the subapical region in adjacent Müller glial cells.

Our *CRB* vectors targeting Müller glial cell and photoreceptors are promising vectors and should be further analyzed for use as clinical grade gene therapy vector. As mutations in the *CRB1* gene not only lead to RP but also to LCA, *CRB* vectors could be tested for their potential in *CRB1*-LCA mouse models (13) to determine their ability to ameliorate the severe retinal disorganization in these mouse models.

Materials and Methods

Generation and purification of the viral vectors

The pAAV2-*GFP* plasmids were generated previously (31) and consist of the flanking inverted terminal repeats (ITRs) of AAV2, the full-length CMV promoter, the engineered and minimal 0.26 Kb CMV promoter which shows similar tropism that native CMV promoter (22) or the GRK1 promoter (25), the *eGFP* cDNA, the woodchuck post-transcriptional regulatory element and the SV40 poly-adenylation sequence. The pAAV2-*CRB1* or pAAV2-*CRB2* plasmids consist of the flanking ITRs of AAV2, the minimal CMV (driving *CRB1* expression), full-length CMV (driving *CRB2* expression) or the human GRK1 promoters, the human codon optimized *CRB1* or *CRB2* cDNA, with a synthetic and short intron sequence and a 48 bp synthetic poly-adenylation sequence. Promoters, cDNA and poly-adenylation sequence were synthesized at Genscript and subcloned in pAAV vectors containing ITRs via Bgl II restriction sites. AAV stocks were generated and purified as previously described (22,31). Briefly, pAAV2 transgene plasmids were co-transfected with the pHelper and pXX2-ShH10F or pAAV9 capsid plasmid into HEK293T cells to generate AAV2/ShH10Y or AAV2/9 viral particles. After DNase treatment, the lysates were ultra-centrifuged onto an iodixanol density gradient (Sigma, St Louis, MO, USA). All viral titers were determined by quantitative PCR and all viral stocks with titers around 1×10^{13} genome copies per ml were stored at −80°C. The AAV6-derived AAV2/ShH10Y445F or ShH10Y serotype showed increased ability to transduce rat and mouse Müller glial cells after intravitreal injection (22,32).

AAV injections

Animal care and use of mice was in accordance with the ARVO statement for the use of animals in ophthalmic and vision research and protocols approved by the Animal Care and Use Committee of the Royal Netherlands Academy of Arts and Sciences (KNAW). The absence of *rd8* and *Pde6b* mutations in all mouse colonies used was tested by PCR. *Crb1*$^{-/-}$, *Crb1*$^{-/-}$*Crb2*$^{F/+}$ Chx10*CreGFP*$^{Tg/+}$ (*Crb1Crb2*$^{F/+}$ cKO), *Crb2*$^{F/F}$ and *Crb2*$^{F/F}$ Chx10 *CreGFP*$^{Tg/+}$ (*Crb2* cKO) mice were generated previously (4,6,10,11). All Chx10*CreGFP*$^{Tg/+}$ or cKO animals display CreGFP expression in retinal progenitors followed by expression in only bipolar cells in post-developmental retinas due to the Chx10 promoter. *Crb2*$^{F/F}$ mice did not express *Cre* and therefore expressed endogenous levels of mouse Crb1 and Crb2. Chromosomal DNA isolation and genotyping were performed as previously described (6). The mice were maintained on a 99.9% C57BL/6J genetic background (except for *Crb1Crb2*$^{F/+}$ cKO injected with AAV2/9-CMV-CRB2 in a 75% C57BL/6J and 25% 129/Ola) on a 12 h day/night cycle and supplied with food and water *ad libitum*. For expression experiments, Post-natal day (P)21 *Crb1*$^{-/-}$ or *Crb2* cKO mice were anesthetized with 100 mg/kg ketamine and 5 mg/kg xylazine intraperitoneally and the pupils were dilated using atropine drops (5 mg/mL). *Crb1*$^{-/-}$ or *Crb2* cKO mice were injected with the AAV-*CRB1 or* AAV-*CRB2* respectively either subretinally or intravitreally as previously described (22,31) with 1 µl of 5.10^9 to 2.10^{10} genome copies of each AAV. Three weeks after injection, the eyes were collected. For rescue experiments, after anesthesia and dilatation of the iris of P14 *Crb1Crb2*$^{F/+}$ or *Crb2* cKO mice, one eye was injected with the AAV-*CRB* (with or without 1/10 diluted GFP virus) and the contralateral eye with the AAV-GFP either subretinally or intravitreally with 1 µl of 5.10^9 to 2.10^{10} genome copies of each AAV. As *Crb1Crb2*$^{F/+}$ cKO retinas are affected only in the inferior but not superior areas (4), the inferior retina was targeted for subretinal injections. The ipsilateral side was either right or left eye in order to prevent bias in the injection or recording. For systemic injections, P2–5 pups were injected in the right retro-orbital sinus ipsilateral (33) with 10–20 µl of 10^{10} genome copies of each AAV. After injection, eyes were treated with chloramphenicol ointment and mice were kept on a heating pad until they fully recovered from anesthesia. Mice were weaned at P21 and *in vivo* experiments were performed at 3, 4 or 5 months.

Eyes injected with AAV-*GFP*, independently of the AAV serotypes and the route of injection used, at doses similar as the eyes injected with AAV-*CRB*, showed no signs of toxicity in comparison to non-injected eyes (Supplementary Material, Fig. S6A–C). Therefore, they are the most appropriate controls to compare with *CRB*-injected eyes.

Electroretinogram (ERG) recordings

Crb1Crb2$^{F/+}$ cKO, *Crb2*$^{F/F}$ and *Crb2* cKO mice were analyzed for retinal activity using another ERG set-up (e.g. using LEDs for stimulation) than used in previous of our reports (4,10), resulting in significant lower amplitudes than previously described for the mixed 50% C57BL/6J- 50% 129/Ola mouse background. Mice from 3 months (M), 4 or 5 M were anesthetized using 100 mg/kg ketamine and 10 mg/kg xylazine intraperitoneally and the pupils were dilated using atropine drops (5 mg/mL). Electroretinograms were recorded for retinal function using the NI622X set-up (National Instrument) with the mouse Ganzfeld bowl inserted in a Faraday cage and signals were amplified using the amplifier model 1700 (A-M systems) with a cut-off of 0.1–20 kHz. A reference electrode was applied subcutaneously in the scalp of the animal, the ground electrode was placed inside the Faraday cage and ipsilateral and contralateral eyes were recorded simultaneously with Ag/AgCl hook electrodes (obtained by chloriding a silver wire in common household bleach) placed on the cornea and methocel drops added (CIBA Vision). Single royal blue (450 nm)-flash responses were obtained under scotopic (dark-adapted overnight) and photopic (light-adapted with a background illumination of 20 cd/m^2 with green (555 nm) LED starting 10 min before recording) conditions. Twenty or ten responses of flash stimuli ranged from −3 to 1.5 log cd s/m^2 under scotopic or photopic respectively, with inter-stimulus intervals of 2.1 s were averaged. ERG analysis was performed using MATLAB and oscillatory potentials (inner layer mainly inhibitory neurons) were normalized to determine a-wave (photoreceptors), b-wave (inner layer mainly bipolar cells). In scotopic b-wave maximum amplitude reached a plateau at −0.5 to 0 log cd s/m^2, which were used to compare *CRB*- or *GFP*-injected eyes and slowly decreased at higher intensities due to unregenerated photopigments. For retro-orbital injection in rescue experiments, only the contralateral (left) eyes were used for analysis. The high variability in ERG responses resulted from the litters, the individual variation in phenotype, the LED performance and the route of injection.

Immunohistochemical analysis

Enucleated eyes were fixed for 30 min in 4% paraformaldehyde in PBS (Phosphate Buffer saline 1×, pH 7.4) and cryoprotected by subsequent incubations of 30 min in 5 and 30% sucrose in PBS. The eyes were embedded in Tissue-Tek (Sakura, Zoeterwoude, The Netherlands), frozen and stored at −20°C. Sections of 7–10 µm were generated with a Leica CM3050 cryostat (Leica Microsystems, Rijswijk, The Netherlands). Sections for immunohistochemistry were blocked for 1 h in 10% normal goat serum, 0.4% Triton X-100 and 1% bovine serum albumin (BSA) in PBS, incubated in a moist-chamber overnight (at 4°C) or 2 h at room temperature with appropriate primary antibodies (Supplementary Material, Table S1) diluted in 0.3% normal goat serum, 0.4% Triton X-100 and 1% BSA in PBS. After rinsing in PBS the sections were incubated for 1 h with Cy3-conjugated goat secondary antibodies anti-mouse or anti-rabbit and rinsed in PBS again. Sections were mounted in Vectashield HardSet DAPI mounting media (Vector Laboratories). Images were generated on a Leica DMRE fluorescence microscope and a Leica SP5 confocal laser scanning microscope and analyzed with Adobe Photoshop CS4.

Eye measurements (perimeters, ciliary body and iris) were done on the largest eye section (comprising or near the optic nerve) of four different animals and averaged. ONL thickness was measured around 1 mm apart from the optic nerve and averaged between the different animals and injected areas. The number of cells in the ganglion cell layer was quantified on the biggest eye section (comprising or near the optic nerve), divided by the length of retina and averaged between the four different animals.

Immuno-electron microscopy

This study was performed in agreement with the declaration of Helsinki on the use of human material for research. Post-mortem human donor eyes (from 40 to 85 years-old donors) were acquired from the Euro Cornea Bank and were processed within 48 h after death. Retinas were dissected from the eyecup and the vitreous was removed and fixed with 4% paraformaldehyde in 0.1 M cacodylate buffer pH 7.4. Immuno-electron microscopy was performed as previously described (4). Briefly, retinas were incubated with the appropriate first antibody for 48 h (Supplementary Material, Table S1), then incubated with secondary anti-rabbit coupled to peroxidase anti peroxidase (PAP) complex 24 h, then developed in a 2,2-diaminobenzidine solution containing 0.03% H_2O_2 for 4 min and then the gold substitute silver peroxidase method was applied. Sections were embedded in epoxy resin, ultrathin sections made, and examined with an electron microscope (FEI Tecnai 12; Fei Company, Eindhoven, The Netherlands).

Statistical analysis

Statistical significance was calculated by using Student′s *t*-test of 3–7 independent retinas. Values were expressed as mean ± s.e.m and $n = 3$–7/condition. Calculations and graphs were generated using GraphPad Prism 5. MANOVA was calculated to compare GFP versus CRB1-injected eyes for seven different measurements relating to eye morphology using four independent retinas per group. The Multivariate test carried out was Wilks′ Lambda. Subsequent Univariate tests were carried out to then look at between subject effects with *P*-value and Partial Eta reported for significance and effect size subsequently. Calculations generated using IBM SPSS Statistics **20**. Values of $^{*}P < 0.05$, $^{**}P < 0.01$, $^{***}P < 0.001$ and $^{****}P < 0.0001$ were considered to be statistically significant.

Supplementary Material

Supplementary Material is available at *HMG* online.

Acknowledgements

The authors thank Rousjan Amir and Thilo M. Buck for contributing data and Dr Sophie van der Sluis for statistical analysis.

Conflict of Interest statement. The authors have the following interests. The Royal Netherlands Academy of Arts and Sciences (KNAW) is owner and L.P.P. and J.W. are the inventors on a patent application related to gene therapy. There are no further patents, products in development or marketed products to declare. This does not alter the authors' adherence to all the journal policies on sharing data and materials, as detailed online in the guide for authors.

Funding

This work was supported by Rotterdamse Vereniging Blindenbelangen, Landelijke St. voor Blinden en Slechtzienden, St. Blindenhulp, St. Oogfonds Nederland, St. Retina Nederland, Netherlands Institute for Neuroscience, Foundation Fighting Blindness USA

(TA-GT-0811-0540-NIN and TA-GT-0313-0607-NIN), and The Netherlands Organization for Health Research and Development (ZonMw grant 43200004 to J.W.), European Union (HEALTH-F2-2008-200234 to J.W.). The funders had no role in study design, data collection and analysis, decision to publish or preparation of the manuscript.

References

1. Alves, C.H., Pellissier, L.P. and Wijnholds, J. (2014) The CRB1 and adherens junction complex proteins in retinal development and maintenance. *Prog. Retin. Eye Res.*, **40**, 35–52.
2. Tsang, S.H., Burke, T., Oll, M., Yzer, S., Lee, W., Xie, Y.A. and Allikmets, R. (2014) Whole exome sequencing identifies CRB1 defect in an unusual maculopathy phenotype. *Ophthalmology*, **121**, 1773–1782.
3. Bujakowska, K., Audo, I., Mohand-Saïd, S., Lancelot, M.E., Antonio, A., Germain, A., Léveillard, T., Letexier, M., Saraiva, J.P., Lonjou, C. *et al.* (2012) CRB1 mutations in inherited retinal dystrophies. *Hum. Mutat.*, **33**, 306–315.
4. Pellissier, L.P., Lundvig, D.M., Tanimoto, N., Klooster, J., Vos, R. M., Richard, F., Sothilingam, V., Garcia Garrido, M., Le Bivic, A., Seeliger, M.W. *et al.* (2014) CRB2 acts as a modifying factor of CRB1-related retinal dystrophies in mice. *Hum. Mol. Genet.*, **23**, 3759–3771.
5. van Rossum, A.G., Aartsen, W.M., Meuleman, J., Klooster, J., Malysheva, A., Versteeg, I., Arsanto, J.P., Le Bivic, A. and Wijnholds, J. (2006) Pals1/Mpp5 is required for correct localization of Crb1 at the subapical region in polarized Muller glia cells. *Hum. Mol. Genet.*, **15**, 2659–2672.
6. van de Pavert, S.A., Kantardzhieva, A., Malysheva, A., Meuleman, J., Versteeg, I., Levelt, C., Klooster, J., Geiger, S., Seeliger, M.W., Rashbass, P. *et al.* (2004) Crumbs homologue 1 is required for maintenance of photoreceptor cell polarization and adhesion during light exposure. *J. Cell Sci.*, **117**, 4169–4177.
7. van de Pavert, S.A., Sanz, A.S., Aartsen, W.M., Vos, R.M., Versteeg, I., Beck, S.C., Klooster, J., Seeliger, M.W. and Wijnholds, J. (2007) Crb1 is a determinant of retinal apical Müller glia cell features. *Glia*, **55**, 1486–1497.
8. van de Pavert, S.A., Meuleman, J., Malysheva, A., Aartsen, W. M., Versteeg, I., Tonagel, F., Kamphuis, W., McCabe, C.J., Seeliger, M.W. and Wijnholds, J. (2007) A single amino acid substitution (Cys249Trp) in Crb1 causes retinal degeneration and deregulates expression of pituitary tumor transforming gene Pttg1. *J. Neurosci.*, **27**, 564–573.
9. Mehalow, A.K., Kameya, S., Smith, R.S., Hawes, N.L., Denegre, J.M., Young, J.A., Bechtold, L., Haider, N.B., Tepass, U., Heckenlively, J.R. *et al.* (2003) CRB1 is essential for external limiting membrane integrity and photoreceptor morphogenesis in the mammalian retina. *Hum. Mol. Genet.*, **12**, 2179–2189.
10. Alves, C.H., Sanz, A.S., Park, B., Pellissier, L.P., Tanimoto, N., Beck, S.C., Huber, G., Murtaza, M., Richard, F., Sridevi Gurubaran, I. *et al.* (2013) Loss of CRB2 in the mouse retina mimics human Retinitis Pigmentosa due to mutations in the CRB1 gene. *Hum. Mol. Genet.*, **22**, 35–50.
11. Alves, C.H., Bossers, K., Vos, R.M., Essing, A.H., Swagemakers, S., van der Spek, P.J., Verhaagen, J. and Wijnholds, J. (2013) Microarray and morphological analysis of early postnatal CRB2 mutant retinas on a pure C57BL/6J genetic background. *PLoS One*, **8**, e82532.
12. Alves, C.H., Pellissier, L.P., Vos, R.M., Garcia Garrido, M., Sothilingam, V., Seide, C., Beck, S.C., Klooster, J., Furukawa, T., Flannery, J.G. *et al.* (2014) Targeted ablation of Crb2 in photoreceptor cells induces retinitis pigmentosa. *Hum. Mol. Genet.*, **23**, 3384–3401.
13. Pellissier, L.P., Alves, C.H., Quinn, P.M., Vos, R.M., Tanimoto, N., Lundvig, D.M., Dudok, J.J., Hooibrink, B., Richard, F., Beck, S.C. *et al.* (2013) Targeted ablation of Crb1 and Crb2 in retinal progenitor cells mimics leber congenital amaurosis. *PLoS Genet.*, **9**, e1003976.
14. Maguire, A.M., Simonelli, F., Pierce, E.A., Pugh, E.N. Jr, Mingozzi, F., Bennicelli, J., Banfi, S., Marshall, K.A., Testa, F., Surace, E. M. *et al.* (2008) Safety and efficacy of gene transfer for Leber's congenital amaurosis. *N. Engl. J. Med.*, **358**, 2240–2248.
15. Bainbridge, J.W., Smith, A.J., Barker, S.S., Robbie, S., Henderson, R., Balaggan, K., Viswanathan, A., Holder, G.E., Stockman, A., Tyler, N. *et al.* (2008) Effect of gene therapy on visual function in Leber's congenital amaurosis. *N. Engl. J. Med.*, **358**, 2231–2239.
16. Hauswirth, W.W., Aleman, T.S., Kaushal, S., Cideciyan, A.V., Schwartz, S.B., Wang, L., Conlon, T.J., Boye, S.L., Flotte, T.R., Byrne, B.J. *et al.* (2008) Treatment of leber congenital amaurosis due to RPE65 mutations by ocular subretinal injection of adeno-associated virus gene vector: short-term results of a phase I trial. *Hum. Gene Ther.*, **19**, 979–990.
17. MacLaren, R.E., Groppe, M., Barnard, A.R., Cottriall, C.L., Tolmachova, T., Seymour, L., Clark, K.R., During, M.J., Cremers, F.P., Black, G.C. *et al.* (2014) Retinal gene therapy in patients with choroideremia: initial findings from a phase 1/2 clinical trial. *Lancet*, **383**, 1129–1137.
18. Alkuraya, F., King Khaled Eye Specialist Hospital. Trial of Ocular Subretinal Injection of a Recombinant Adeno-Associated Virus (rAAV2-VMD2-hMERTK) Gene Vector to Patients With Retinal Disease Due to MERTK Mutations. http://clinicaltrials.gov/show/NCT01482195.
19. Rakoczy, P.E., Lions Eye Institute, Perth, Western Australia. Safety and Efficacy Study of rAAV.sFlt-1 in Patients With Exudative Age-Related Macular Degeneration (AMD). http://clinicaltrials.gov/ct2/show/NCT01494805.
20. Sanofi-Genzyme. Safety and Tolerability Study of AAV2-sFLT01 in Patients With Neovascular Age-Related Macular Degeneration (AMD). http://clinicaltrials.gov/ct2/show/NCT01024998.
21. Lipinski, D.M., Thake, M. and MacLaren, R.E. (2013) Clinical applications of retinal gene therapy. *Prog. Retin. Eye Res.*, **32**, 22–47.
22. Pellissier, L.P., Hoek, R.M., Vos, R.M., Aartsen, W.M., Klimczak, R.R., Hoyng, S.A., Flannery, J.G. and Wijnholds, J. (2014) Specific tools for targeting and expression in Müller glial cells. *Mol. Ther. — Meth. Clin. Dev.*, **1**, 14009.
23. Bostick, B., Ghosh, A., Yue, Y., Long, C. and Duan, D. (2007) Systemic AAV-9 transduction in mice is influenced by animal age but not by the route of administration. *Gene Ther.*, **14**, 1605–1609.
24. Dalkara, D., Byrne, L.C., Lee, T., Hoffmann, N.V., Schaffer, D.V. and Flannery, J.G. (2012) Enhanced gene delivery to the neonatal retina through systemic administration of tyrosine-mutated AAV9. *Gene Ther.*, **19**, 176–181.
25. Khani, S.C., Pawlyk, B.S., Bulgakov, O.V., Kasperek, E., Young, J.E., Adamian, M., Sun, X., Smith, A.J., Ali, R.R. and Li, T. (2007) AAV-mediated expression targeting of rod and cone photoreceptors with a human rhodopsin kinase promoter. *Invest. Ophthalmol. Vis. Sci.*, **48**, 3954–3961.
26. Zou, J., Wang, X. and Wei, X. (2012) Crb apical polarity proteins maintain zebrafish retinal cone mosaics via intercellular binding of their extracellular domains. *Dev. Cell*, **22**, 1261–1274.
27. Hsu, Y.C. and Jensen, A.M. (2010) Multiple domains in the Crumbs Homolog 2a (Crb2a) protein are required for regulating rod photoreceptor size. *BMC Cell Biol.*, **11**, 60.

28. Willett, K. and Bennett, J. (2013) Immunology of AAV-Mediated Gene Transfer in the Eye. *Front. Immunol.*, **4**, 261.
29. van den Hurk, J.A., Rashbass, P., Roepman, R., Davis, J., Voesenek, K.E., Arends, M.L., Zonneveld, M.N., van Roekel, M.H., Cameron, K., Rohrschneider, K. *et al.* (2005) Characterization of the Crumbs homolog 2 (CRB2) gene and analysis of its role in retinitis pigmentosa and Leber congenital amaurosis. *Mol. Vis.*, **11**, 263–273.
30. Greenberg, K.P., Geller, S.F., Schaffer, D.V. and Flannery, J.G. (2007) Targeted transgene expression in muller glia of normal and diseased retinas using lentiviral vectors. *Invest. Ophthalmol. Vis. Sci.*, **48**, 1844–1852.
31. Aartsen, W.M., van Cleef, K.W., Pellissier, L.P., Hoek, R.M., Vos, R.M., Blits, B., Ehlert, E.M., Balaggan, K.S., Ali, R.R., Verhaagen, J. *et al.* (2010) GFAP-driven GFP expression in activated mouse Müller glial cells aligning retinal blood vessels following intravitreal injection of AAV2/6 vectors. *PLoS One*, **5**, e12387.
32. Klimczak, R.R., Koerber, J.T., Dalkara, D., Flannery, J.G. and Schaffer, D.V. (2009) A novel adeno-associated viral variant for efficient and selective intravitreal transduction of rat Müller cells. *PLoS One*, **4**, e7467.
33. Yardeni, T., Eckhaus, M., Morris, H.D., Huizing, M. and Hoogstraten-Miller, S. (2011) Retro-orbital injections in mice. *Lab. Anim. (NY)*, **40**, 155–160.